Supporting Information for Electronic State-Resolved Electron-Phonon Coupling in an Organic Charge Transfer Material from Broadband Quantum Beat Spectroscopy

Aaron S. Rury, Shayne Sorenson, Eric Driscoll, and Jahan M. Dawlaty*

Department of Chemistry, University of Southern California

E-mail: arury@usc.edu

S1. Steady-State Spectrum of Quinhydrone

Figure S1 compares the steady-state reflectance spectrum of quinhydrone as seen in Ref. [1] to that 2.64 eV pump and white light continuum probe.[1]

S2. Broadband Transient Reflectivity Spectra

Top panels of figures 2 and 3 show the broadband resonant transient reflectivity (rTR) and non-resonant transient reflectivity spectra, respectively, of single monoclinic quinhydrone crystals. Also the bottom panels show the same representative kinetic traces as seen in the main manuscript for the reader's reference. The pump and probe pulses are polarized along the a-axis of the crystal and we have not corrected the spectrum for the chirp of the probe pulse, which causes higher probe energies to reach the sample before those of lower energy

*To whom correspondence should be addressed

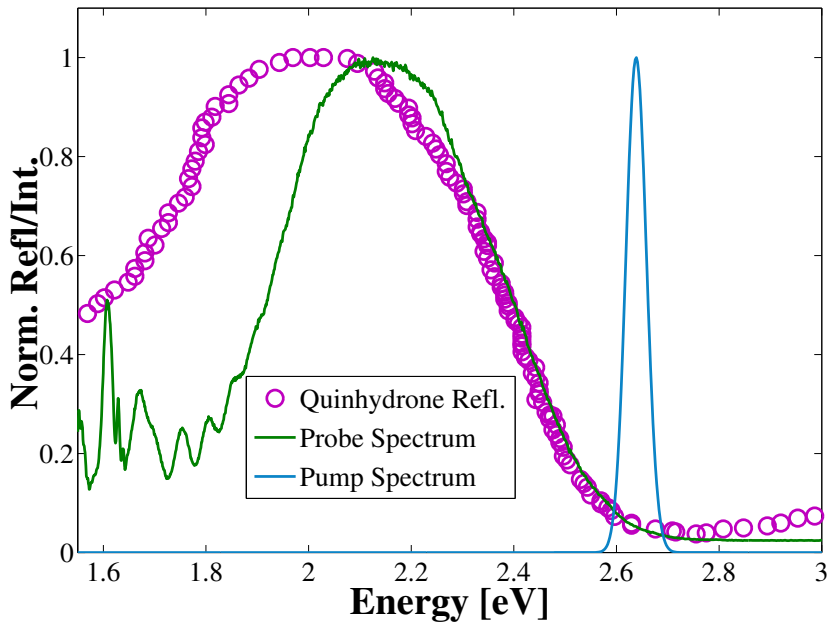

Figure 1: Comparison of the normalized reflectance of monoclinic quinhydrone crystals taken from Ref. [1] (purple) compared to the normalized intensity profiles of the 2.64 eV pump (light blue) and white light continuum probe (red) pulses.

S3. Singular Value Decomposition Analysis

As stated in the manuscript, the singular value decomposition (SVD) algorithm decomposes the raw data matrix $\mathbf{A}$(t,λ) as

$$\mathbf{A}(t, E) = \mathbf{U}(t)\mathbf{S}\mathbf{V}(E)^{\dagger}, \tag{1}$$

where $\mathbf{S}$ contains the singular values, or weights, with which the components of the matrices $\mathbf{U}$(t) and $\mathbf{V}$(E) contribute to the raw data. As implied by the variables in parenthesis, $\mathbf{U}$(t) and $\mathbf{V}$(E) decompose the data into time domain and frequency domain vector spaces, respectively. The number of components used for the analysis undertaken in the manuscript is set by the ratio of the singular value of a given component to that of the largest singular value. For the case of the resonant transient reflectivity (rTR) spectrum shown in Figure 2, we used three SVD components since the ratio of the fourth singular value to the first was

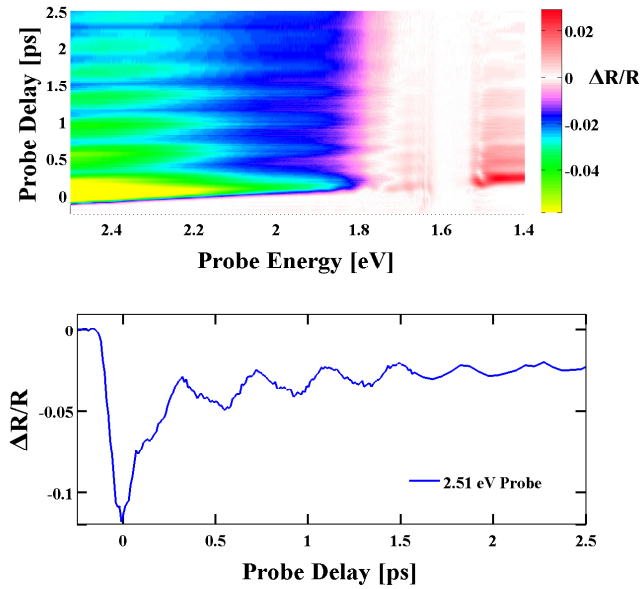

Figure 2: Top: Broadband ultrafast resonant transient reflectivity (TR) spectrum of monoclinic quinhydrone over the first 2.5 ps of probe delay after the sample is excited at 2.64 eV probed in the band of 1.4 eV to 2.5 eV. Large amplitude oscillations appear in the spectra as horizontal stripes demonstrating coherent excitation of the crystal lattice by the ultrafast electron transfer. Bottom: Kinetic slice of the rTR spectra taken at a probe energy of 2.5 eV showing representative oscillations observed across the rTR spectrum.

less than 0.05. That is, the ratios of **S**(2,2) and **S**(3,3) to **S**(1,1) are both larger than 0.05, while that of **S**(4,4) is not. Figure 4 shows the amplitude of the first three components of **U**(t) and **V**(E)† weighted to their associated singular value. In the case of the impulsive stimulated Raman scattering (ISRS) spectrum shown in the top panel of Figure 3 above, five singular values fit the criteria used above, i.e. **S**(n,n)/**S**(1,1)>0.05. These components are shown in Figure

S4. Wider Spectral Span Fourier Spectra

Figure 6 shows the weighted fast Fourier transforms of the rTR (blue) and rTR (green) measurements for Fourier frequencies of 40 cm^{-1} to 500 cm^{-1}.

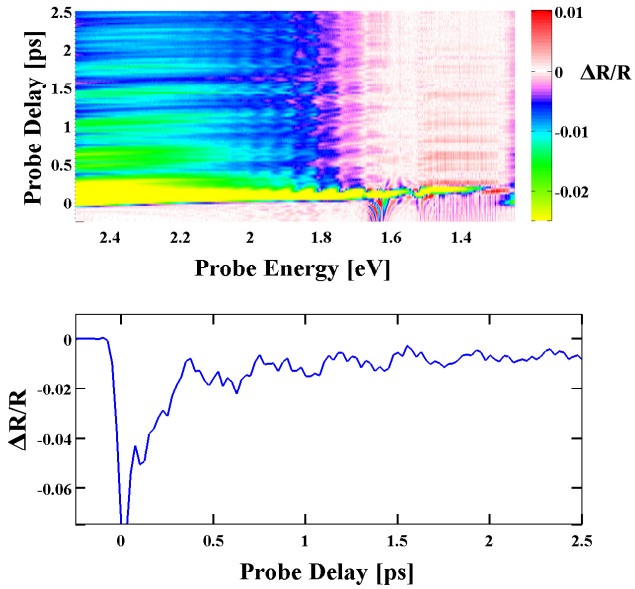

Figure 3: Top: Broadband ultrafast non-resonant transient reflectivity (nrTR) spectrum of monoclinic quinhydrone over the first 2.5 ps of probe delay after the sample is excited at 0.95 eV probed in the band of 1.25 eV to 2.5 eV.. Ground state oscillations driven by impulsive stimulated Raman scattering appear as horizontal stripes, similarly to those observed in the top panel of Figure 2. Bottom: Kinetic slice of the nrTR spectra taken at a probe energy of 2.48 eV showing representative oscillations observed across the nrTR spectrum.

S5. Calculation of Fourier and electron-phonon coupling spectra from SVD components

Using the components of the SVD analysis that meet the criteria above, we then determine their frequency content via Fourier transform of the dynamical matrix **U**(t). This allows direct comparison to rR spectra and calculation of the electron-phonon (e-ph) coupling spectra shown in Figure 4 of the manuscript. To best approximate the frequency composition of the measured data, these Fourier transformed traces must be weighted by their associated singular values. That is, the Fourier spectrum associated with the nth component **U**(t) becomes,

$$F^n(\omega) = FT[U^n(t)]S(n,n), \tag{2}$$

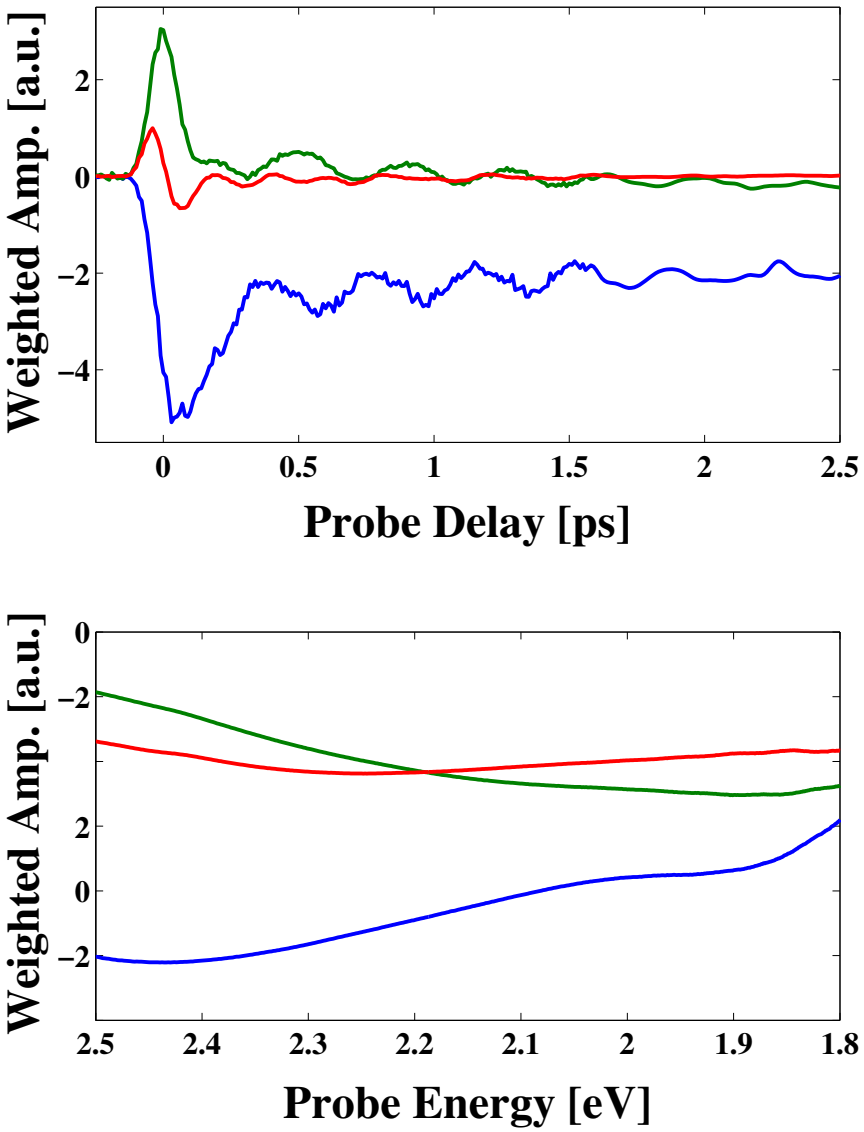

Figure 4: Top: Singular value-weighted first (blue), second (green) and third (red) components of the $\mathbf{U}(t)$ matrix derived from the resonant Transient Reflectivity spectrum of monoclinic quinhydrone single crystals excited at 2.64 eV. Bottom: Singular value-weighted first (blue), second (green) and third (red) components of the $\mathbf{V}(E)^{\dagger}$ matrix derived from the same data as the top panel.

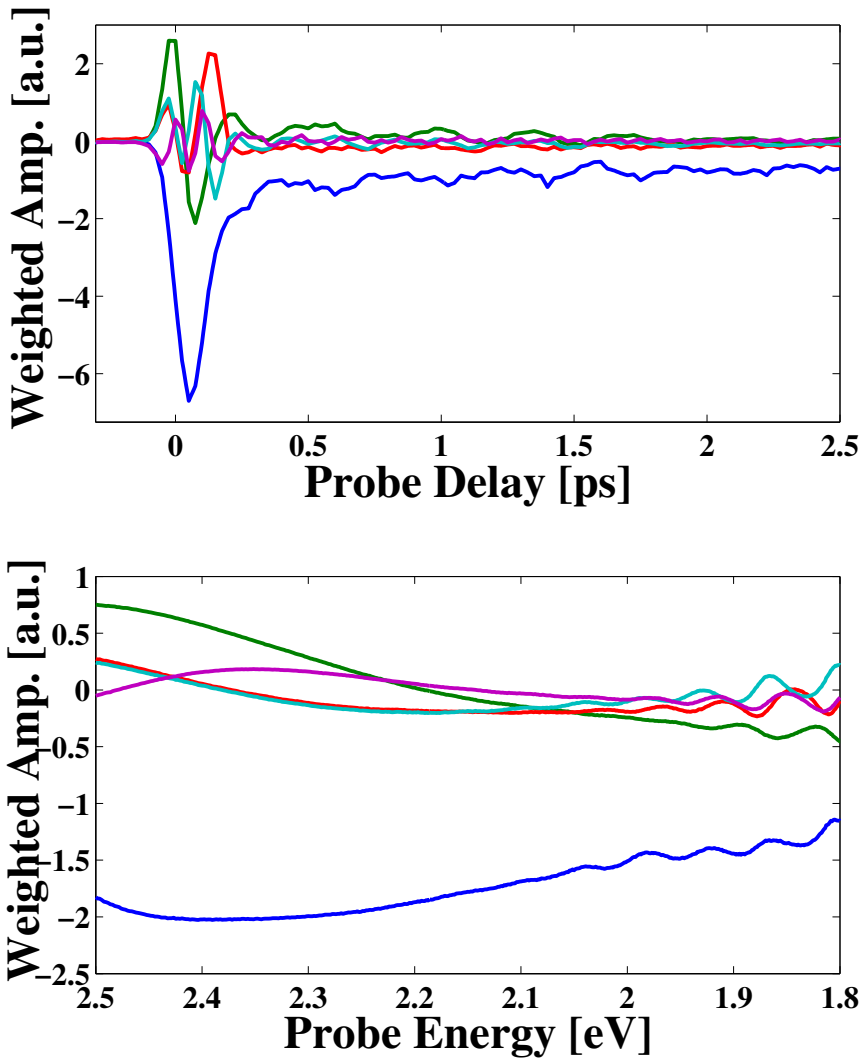

Figure 5: Top: Singular value-weighted first (blue), second (green) and third (red) components of the $\mathbf{U}(t)$ matrix derived from the impulsive stimulate Raman scattering spectrum of monoclinic quinhydrone single crystals excited at 0.95 eV. Bottom: Singular value-weighted first (blue), second (green) and third (red) components of the $\mathbf{V}(E)^{\dagger}$ matrix derived from the same data as the top panel.

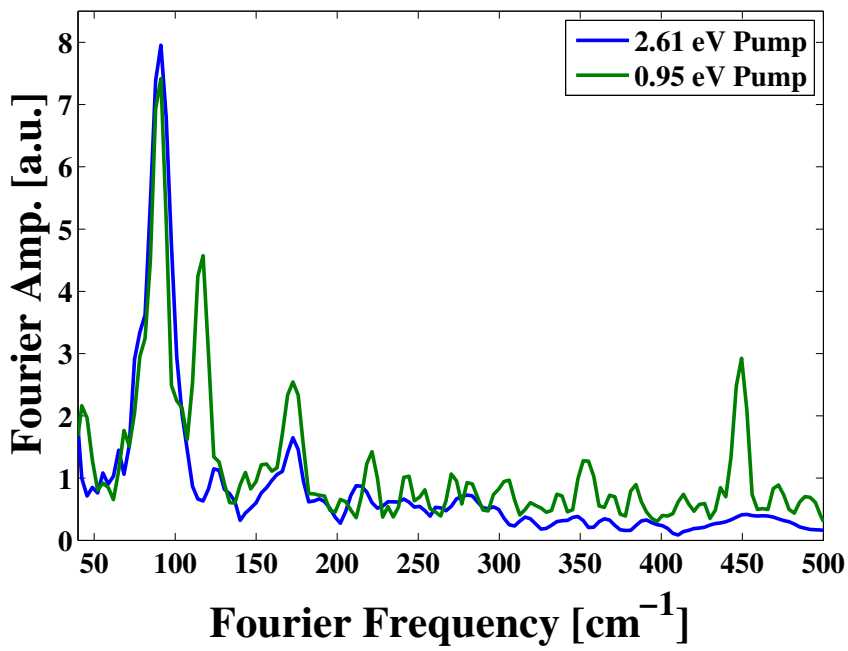

Figure 6: Fourier spectra extracted from the resonant transient reflectivity (blue) and non-resonant reflectivity (green) measurements shown in the spectral window of 50-500 cm^{-1}.

where FT is the Fourier transform operation. To calculate the full Fourier spectrum, as shown in the top panel of Figure 4 of the manuscript, we sum over the appropriate number of components given the criteria outlined in the previous section. Therefore, the Fourier spectrum becomes,

$$\mathbf{F}(\omega) = \sum_n F^n(\omega) = \sum_n FT[U^n(t)]S(n.n) \tag{3}$$

where n=3 and n=5 for the rTR and ISRS spectra, respectively. Once we calculate the Fourier spectrum, the full 2D e-ph coupling spectrum is found by matrix multiplying by spectral components derived from the SVD decomposition,

$$\mathbf{C}(\omega, \lambda) = \mathbf{F}(\omega)\mathbf{V}(E)^{\dagger} \tag{4}$$

To produce spectra like those seen in Figure 5 of the manuscript, one simply extracts the column associated with a particular value of ω of interest and plot its variation as a function of the probe's energy.

This analysis also justifies the lack of a unitary transform of the individual components of U(t). A previous study by Ernsting *et al.*[2] showed that one can 'rotate' the components of the dynamics matrix from SVD of transient absorption data such that each frequency exists in a single component. The transformed dynamical matrix becomes,

$$\mathbf{U}'(t) = \mathbf{U}(t)\mathbf{R}, \tag{5}$$

where $\mathbf{R}$ is a generalized rotation matrix that obeys unitarity. However, in order to conform to the distributive properties of linear algebra, Eq. (1) implies that the raw data remain unchanged such that,

$$\mathbf{A}(t,E) = \mathbf{U}(t)\mathbf{S}\mathbf{V}(E)^{\dagger} = \mathbf{U}'(t)\mathbf{R}\mathbf{R}^{-1}\mathbf{S}\mathbf{V}(E)^{\dagger}. \tag{6}$$

Under such a rotation the Fourier spectrum becomes,

$$\begin{aligned}\mathbf{F}'(\omega) &= \sum_n FT[U'^n(t)]S(n.n) = \sum_n FT[U^n(t)R(n,n)]R^{-1}(n,n)S(n.n) \\ &= \sum_n FT[U^n(t)]R(n,n)R^{-1}(n,n)S(n.n) = \sum_n FT[U^n(t)]S(n.n) = \mathbf{F}(\omega),\end{aligned} \tag{7}$$

since the rotation matrix $\mathbf{R}$ contains no dynamical information. Therefore, both the Fourier spectra and the e-ph coupling spectra shown in Figures 4 and 5, respectively, would remain unchanged under any such unitary transform.

The transformation by $\mathbf{R}$ of the SVD components allows one to make a connection between the spectral and temporal evolution of different components with specific physically distinct species that participate in the ultrafast dynamics of the sample of interest. In the components presented in Figures (4) and (5) we have no such transformation and, therefore,

these components should not inform one's physical interpretation of the dynamical processes taken place in our measurements. However, as shown by Eq. (7), even with the lack of a transformation into a vector space relevant to the physical dynamics of quinhydrone, one can still calculate the e-ph coupling spectrum and assess the coupling of specific phonons with electronic transitions in a spectral region of interest.

S6. Amplitude and Phase of Electron-phonon Coupling Spectra of Quinhydrone

In addition to providing a contrast to e-ph coupling in the electronic excited state of quinhydrone, our ISRS measurements may explain the nature of the electronic state excited by the 2.64 eV pump as well as the reason why the ground state intermolecular phonons of quinhydrone may not couple to optical transitions in the visible region. Figure 7 shows the quantum beat spectrum of the BQ ?6 mode extracted from our nrTR measurements shown in Figure 3. One sees a spectral minimum associated with a phase discontinuity near 2.43 eV, which indicates the presence of an optical transition near this energy that is modulated by this intramolecular vibration. Previous solution phase measurements have shown a group of absorption peaks near 2.5 eV[3] that theoretical studies have proposed to stem from singlet transitions between orbitals delocalized throughout the molecule, including the p orbitals of the oxygens, to delocalized π^* states of the aromatic ring, denoting this transition as $n \rightarrow \pi^*$[4,5] In such a case it would be plausible that coherent intermolecular phonon excitations would not couple to this transition, as we see for both ground state the e-ph coupling spectra of quinhydrone in Figure 5. However, since the $n \rightarrow \pi^*$ transition populates the same molecular orbital of BQ that would accept an electron from HQ in quinhydrone, the optical absorption of the probe pulse after 2.64 eV excitation could transfer an electron from one monomer to the other. Therefore, the excited state e-ph coupling spectrum associated with the ?4 mode and its phase are consistent with the picture that this phonon directly

modulates t in an electronic excited state of quinhydrone.

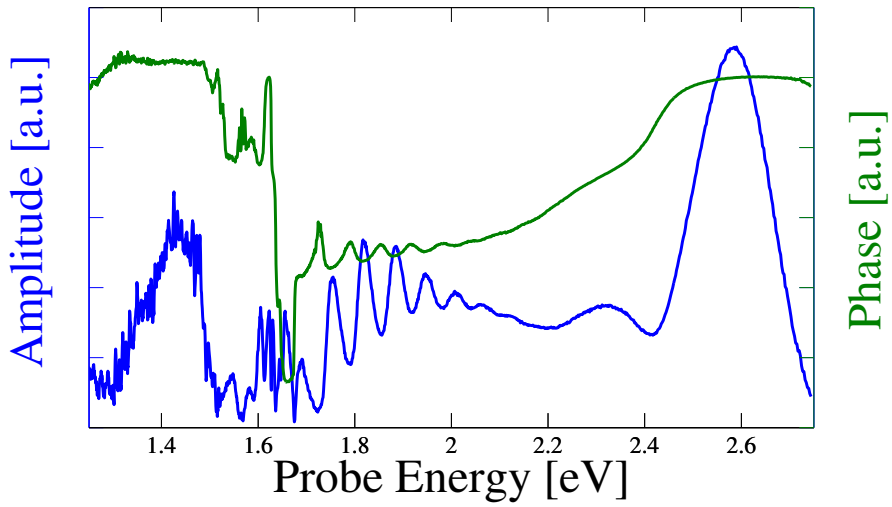

Figure 7: Amplitude (blue) and phase (green) of the electron-phonon coupling spectra of the p-benzoquinone ν_6 mode in the ground state of quinhydrone in the spectral window of 1.35 eV to 2.75 eV.

References

(1) Mitani, T.; Saito, G. *Synthetic Metals* **1988**, *27*, B499–B508.

(2) Ernsting, N. P.; Kovalenko, S. A.; Senyushkina, T.; Saam, J.; Farztdinov, V. *The Journal of Physical Chemistry A* **2001**, *105*, 3443–3453.

(3) Ahmed, M.; Khan, Z. H. *Spectrochimica Acta Part A: Molecular and Biomolecular Spectroscopy* **2000**, *56*, 965–981.

(4) Trommsdorff, H. P. *The Journal of Chemical Physics* **1972**, *56*, 5358.

(5) Pou-Amerigo, R.; Merchan, M.; Orti, E. *Journal of Chemical Physics* **1999**, *110*, 9536–9546.

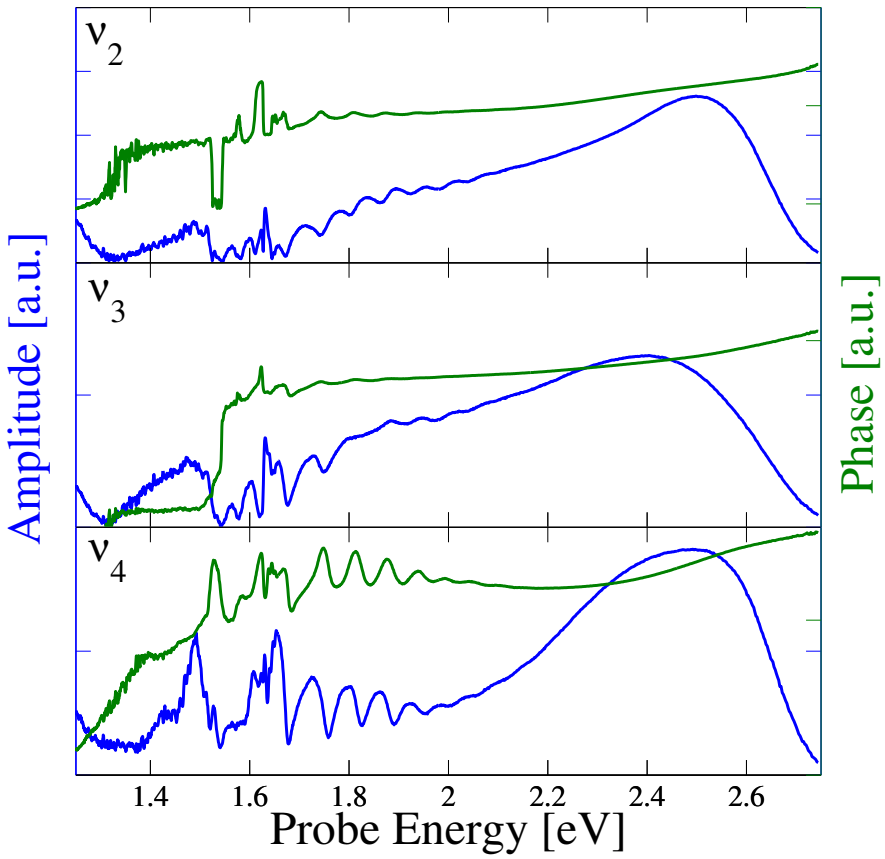

Figure 8: Amplitude (blue) and phase (green) of the electron-phonon coupling spectra of the ν_2 mode (top), ν_3 mode (middle) and ν_4 mode (bottom) in the ground electronic state of quinhydrone in the spectral window of 1.35 eV to 2.75 eV.

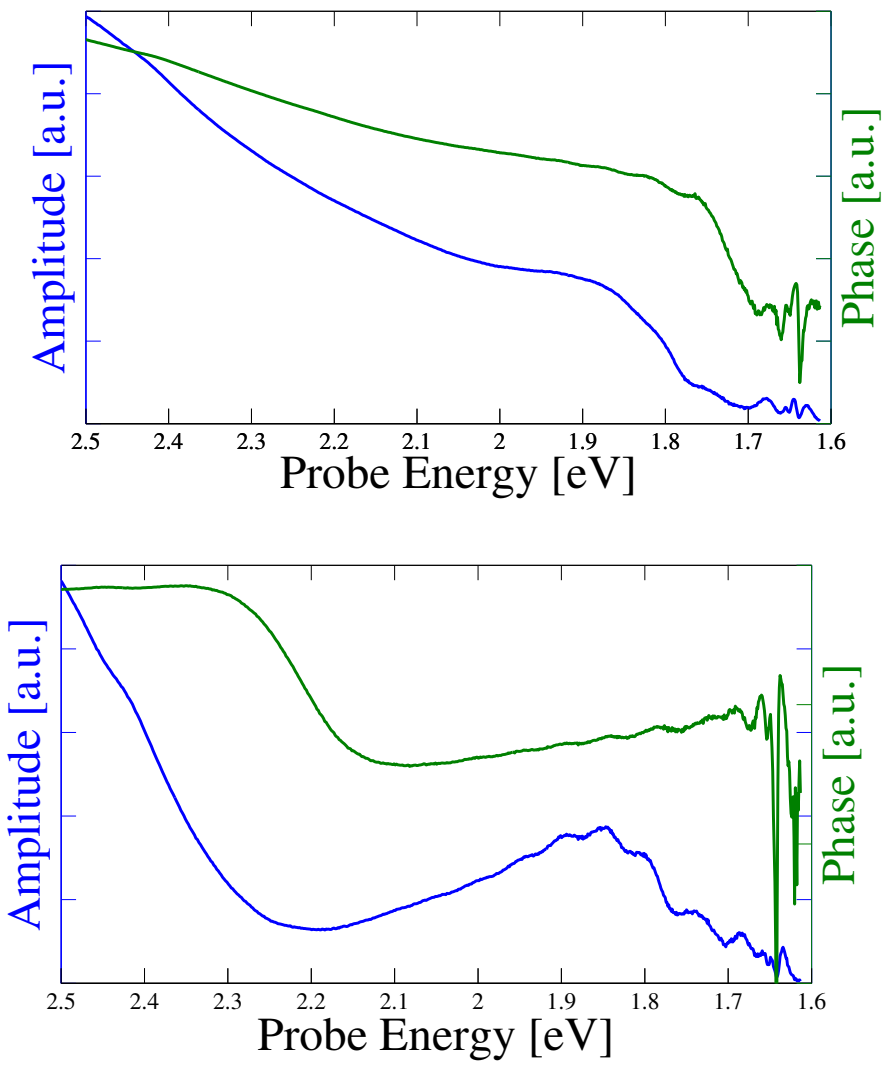

Figure 9: Amplitude (blue) and phase (green) of the electron-phonon coupling spectra of the ν_2 mode (top) and ν_4 mode (bottom) in the excited electronic state of quinhydrone in the spectral window of 1.6 eV to 2.5 eV.